Hindawi
Geofluids
Volume 2021, Article ID 4023704, 15 pages
https://doi.org/10.1155/2021/4023704

Research Article

A New Quantitative Approach for Element-Mineral Determination Based on "EDS (Energy Dispersive Spectroscopy) Method"

Peigang Liu,[1,2] **Zhelin Wang**,[2,3] **and Zhiqiang Zhang**[2]

[1]*College of Computer Science and Technology in China University of Petroleum (East China), Qingdao 266580, China*
[2]*School of Earth and Space Sciences in Peking University, Beijing 100871, China*
[3]*SINOPEC Petroleum Exploration and Production Research Institute, Beijing 100083, China*

Correspondence should be addressed to Peigang Liu; dongfangwy@126.com

Received 7 May 2021; Revised 24 July 2021; Accepted 29 July 2021; Published 29 August 2021

Academic Editor: Yanjun Meng

With the continuous development of hydrocarbon exploration, how to efficiently, economically, accurately, and comprehensively obtain mineral species, composition, and structure and diagenesis information has become one of the hot topics in both the academia and industry. By scanning electron microscopy (SEM) and energy dispersive spectroscopy (EDS), a new method of qualitative mineral identification and quantitative measurement is established. Typical tight sandstone reservoir rock samples in the Ordos Basin are selected; through the element surface scanning image of "mineral element composition" and "pixel element combination", mineral types are distinguished, and mineral parameters such as types, characteristics, and content are rapidly and accurately determined. Meanwhile, such results achieved via the new method are compared with conventional XRD and TIMA methods. The results show that the new method exhibits several advantages: cost advantages compared to XRD experiment analysis technology and TIMA system and ability to analyze low content minerals which XRD techniques are hard to identify; it allows quantitative characterization on the phenomenon of mineral miscibility, which is of great significance to explore the mineral diagenetic evolution.

1. Introduction

The rapid development of oil and gas exploration requires more detailed study of the tight reservoirs. Qualitative analyses and quantitative measurements of mineral compositions within the tight reservoir are of great significance to practical application. The identification of rocks and minerals can provide accurate and comprehensive information including mineral composition and structural characteristics and diagenesis and allows revealing the reservoir heterogeneity and pore structure [1–4].

At present, the methods of qualitative observation of minerals include the optical microscope method, scanning electron microscopy, and infrared spectroscopy [5–7]. The optical microscopy method provides comprehensive analysis of mineral characteristics and mutual relationships. However, because of the limitation of resolution, it can do little in terms of determining the qualitative analysis of small particles, especially micro-nanoscale mineral morphology and structural characteristics [8–10]. The scanning electron microscopy method focuses on the surface morphology of nanometer/micron scale minerals via secondary electronic imaging [11]. The scanning electron microscope and the X-ray methods are often combined to realize the comprehensive analysis of the mineral components and microstructure [12, 13]. The infrared spectrum method is to obtain the structure information of the mineral molecules and obtain composite database by establishing the infrared spectrum diagram. This method has been used to qualitatively characterize the minerals, to study the composition of oil and gas inclusion, and the temperature

of the abundance of the oil and gas [14–18]. The laser Raman spectroscopy provides accurate and rapid measurement of the fluid components in the rock by using the laser Raman spectrometer [19–23]. It is, however, difficult to accurately determine the mineral type and calculate the mineral content, yet it can only analyze the mineral composition elements. Therefore, to make quantitative characterization of minerals/elements, to combine the Raman spectrometer and other methods and instruments has become one of the key development trends of Raman spectroscopy [24–27].

X-ray diffraction (XRD) is the main method for quantitative mineral analysis. According to the positive correlation between diffraction intensity and content of minerals, mineral content in rocks can be rapidly and accurately analyzed [28]. For instance, X-ray diffraction can be used to rapidly analyze the content of calcite and dolomite in carbonate rocks [29], study the order degree of dolomite [30], and identify the minerals in phyllite and kimberlite, so as to evaluate the deposit [31, 32]. However, close symbiosis and associated phenomena of different minerals in rocks exist, and it is susceptible to the influence of diffraction peaks of other minerals when the content of measured minerals is low [33]. In addition, the mineral morphology cannot be directly observed by using the X-ray diffraction method, and the change of some mineral compositional structure could lead to errors in the analysis results [9].

Mineral identification methods that combine qualitative observation with quantitative analysis include mineral dissociation analysis (MLA) [7, 34], quantitative evaluation of minerals by scanning electron microscopy (QEMSCAN), and automatic mineral characterization quantitative analysis system (AMICS) ([6, 35–37]). This method establishes a set of mineral quantitative analysis system through scanning electron microscopy and energy spectrometer and uses the backscattered electron (BSE) image which can reflect the difference of mineral phase composition and X-ray energy spectrum rapid analysis technology to accurately identify minerals [7, 38]. Some scholars used INCA software on OXFORD spectrometer to establish a synthetic energy spectrum database and retrieval system for minerals and used it to identify minerals [39]. Such methods have already realized quantitative identification of rare earth minerals which conventional identification methods are difficult to accomplish, yet problems such as high measurement cost and difficulty in application and promotion still exist [40–48].

Aiming at the existing disadvantages regarding the qualitative identification and quantitative measurements of minerals, the objectives of this paper are to introduce a new method of mineral identification and measurement based on SEM and EDS, and it is named "EDS method." This method allows identification of minerals in the microsurface area using the element surface scanning image of "mineral element composition" and "pixel element combination" and can determine accurately and quickly the mineral types, mineral characteristics, and mineral content. This method also enables qualitative identification and quantitative characterization of minerals that affect pore throat system, and it has been applied to the Triassic Yanchang Formation, Ordos Basin, to analyze the mineral composition and content.

2. Methodology

Existing literature suggests that the rock mineral identification has evolved to a trend that requires both qualitative morphological determination and quantitative structural and principle analyses (e.g., Liao 2018). Accordingly, with the rapid development of equipment, the Fourier infrared spectrometer, X-ray diffractometer, Raman spectrometer, and scanning electron microscope have been applied to mineral identification [6, 9, 34].

The EDS method proposed in this paper is based on surface micro area identification via SEM-EDS image "mineral element composition" and "pixel element association" (Table 1): mineral element association: based on chemical formula discrimination of basic minerals; pixel element association: based on scanning every single pixel "one and only" element association.

The procedures are as follows (Figure 1):

(1) Draw element content distribution map. Samples and local positions are selected, holographic surface scan is run using the OXFORD INCA X-MAX50 250+, and distribution map of basic element composition and element content are generated

(2) Determine pixel element distribution. The distribution map is divided into pixel points, according to the relative mineral element content distribution, and the mineral type of each point is determined

(3) Run new algorithm of mineral identification. Based on the skeleton and element associations of clay minerals, the mineral identification is realized based on "pixel element association" method

(4) Run denoise and correction process. After the mineral type is identified, the skeleton mineral is denoised using the marginal examination method and compared to the original image so that they are in line with the actual situation

On the basis of "mineral element association," "impurity element and substitute element," and "statistics of energy spectrum point," considering all the possible element associations (Table 2), the mineral identification is realized.

In order to achieve a better recognition effect, it is necessary to take full consideration of the "one and only" element combinations at pixel points when using the new method, including (1) the alternative elements that may exist in some mineral element combinations, such as the alternative elements Mg and Fe in kaolinite ($Al_4[Si_4O_{10}](OH)_8$); (2) when the sample is not oil-washed, the influence of element C should be considered due to the existence of residual oil in clay minerals and some skeleton minerals; (3) the analysis should be carried out according to the actual situation of the energy spectrum points of each mineral. In the process of miscibility of different minerals, impurity elements may exist, such as potassium feldspar ($K[AlSi_3O_8]$) and albite ($Na[AlSi_3O_8]$) in the perthite, yet mixing of Ca element may exist.

Table 1: Rock mineral major and associated and impurity element.

Type	Mineral	Chemical formula	Major element	Associated/impurity element
Oxide	Quartz	SiO_2	Si, O	C
Silicates carbonate	Potash feldspar	$K[AlSi_3O_8]$	K, Al, Si, O	Na, C
Silicate	Plagioclase	$Na[AlSi_3O_8]$ $Ca[Al_2Si_2O_8]$	Na/Ca, Al, Si, O	C
Carbonate	Calcite	$Ca[CO_3]$	Ca, C, O	Si, Fe
	Dolomite	$CaMg[CO3]_2$	Ca, Mg, C, O	Si, Fe
	Siderite	$Fe[CO_3]$	Fe, C, O	/
Sulfide	Pyrite	$Fe[S_2]$	Fe, S	C
Silicate	Illite	$K_{0.75}(Al_{1.75}MgFe)[Al_{0.5}Si_{3.5}O_{10}](OH)_2$	K, Mg, Fe, Al, Si, O	Na, C
Silicate	Chlorite	$(Mg_3/Al_3/Fe_3)[Si_4O_{10}](OH)_2$	Mg, Fe, Al, Si, O	C
Silicate	Smectite	$E_x(B2O)_4\{(Al_{2-x},Mg_x)_2[(Si,Al)_4O_{10}](OH)_2\}$	Mg, Al, Si, O	Na, Ca, K, C
Silicate	Kaolinite	$Al_4[Si_4O_{10}](OH)_8$	Al, Si, O	Mg, Fe, C
Pore	Residual oil	C	O	

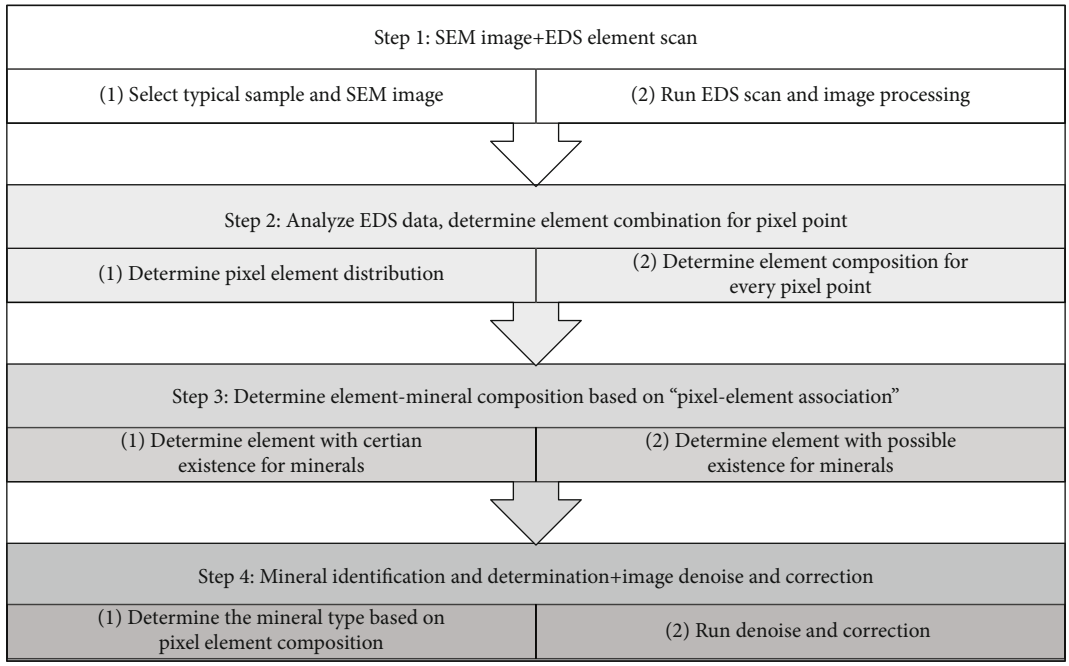

Figure 1: Technical process of EDS element-mineral identification.

3. Results

3.1. SEM-EDS Element Scan Results. Planar scanning is run through the scanning electron beam on the specimen surface observation area, and different element displays on the screen in different colors, respectively, showing the distribution of the image. It can also correspond to acquisition of secondary electron image, which is intuitive and clear—the more points, the higher brightness and thus the higher indicator element content. Although the accuracy of quantitative analysis of light elements by this method is not ideal at present, it is still of practical significance to take the quantitative analysis result as the data of relative comparison. The back and bottom noise of surface scanning will also produce a small amount of bright spots, which cannot be distinguished from low-content elements. The sample surface is required to be smooth, and the thin slice sample after cutting should be selected and treated with soot blowing and cadmium spraying. As shown in Figure 2, the SEM scanning electron microscope image and local mineral characteristics of sample 284-3-9-Z were selected, and EDS holographic scanning was performed.

According to the distribution of holographic scanning results of common elements, the relative contents and areal distribution of K, Na, Ca, Mg, Al, Si, Fe, C, and O were obtained (Figure 3). Then, according to the new SEM-EDS element-mineral determination method, the common skeleton minerals and clay minerals are identified and displayed.

Table 2: Element associations for new mineral identification method.

No.	Minerals	Element with certain existence	Elements with possible existence
1	Quartz	Si, O	C
2	Potash feldspar	K, Al, Si, O	Na, C
3	Albite	Na, Al, Si, O	Ca, C
4	Anorthite	Ca, Al, Si, O	C
5	Calcite	Ca, C, O	Si, Fe
6	Dolomite	Ca, Mg, C, O	Si, Fe
7	Siderite	Fe, C, O	/
8	Pyrite	Fe, S	C
9	1 Illite 1	K, Mg, Fe, Al, Si, O	Na, C
10	2 Illite 2	Na, Mg, Fe, Al, Si, O	K, C
11	Chlorite	Mg, Fe, Al, Si, O	C
12	Smectite	Mg, Al, Si, O	Na, Ca, K, C
13	Kaolinite	Al, Si, O	Fe, C
14	Pore	C	O

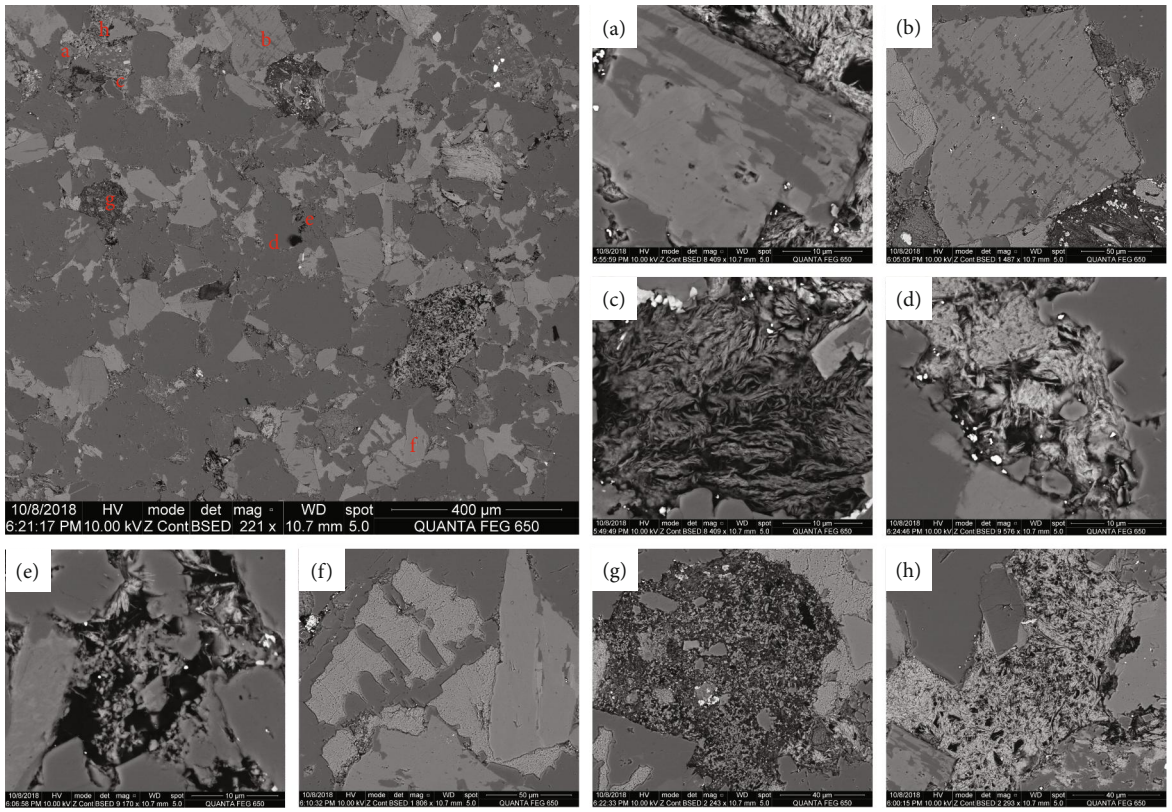

Figure 2: Sample 284-3-9-Z SEM-EDS holographic scanning and local mineral features. (a, b) Miscible potassium and sodium feldspar; (c, d) clay minerals; (e) minerals and pores; (f) dissolved potassium feldspar which is filled with calcite; (g, h) mixed mineral debris in pores.

3.2. Mineral Identification Results and Verification. Based on the element associations and content relationship discussed above, mineral type identification and mineral content determination are realized using the new planar scanning method (Figure 4). First, the major mineral of the selected sample is determined, including the skeleton mineral (quartz, potash feldspar, albite, and carbonate minerals) and clay minerals (illite, chlorite, smectite, kalinite, etc.). In addition, the mineral content planar distribution is analyzed, while the rest represents pores.

The rock skeleton mineral is characterized by smooth and complete surface, such as quartz, potash feldspar, albite,

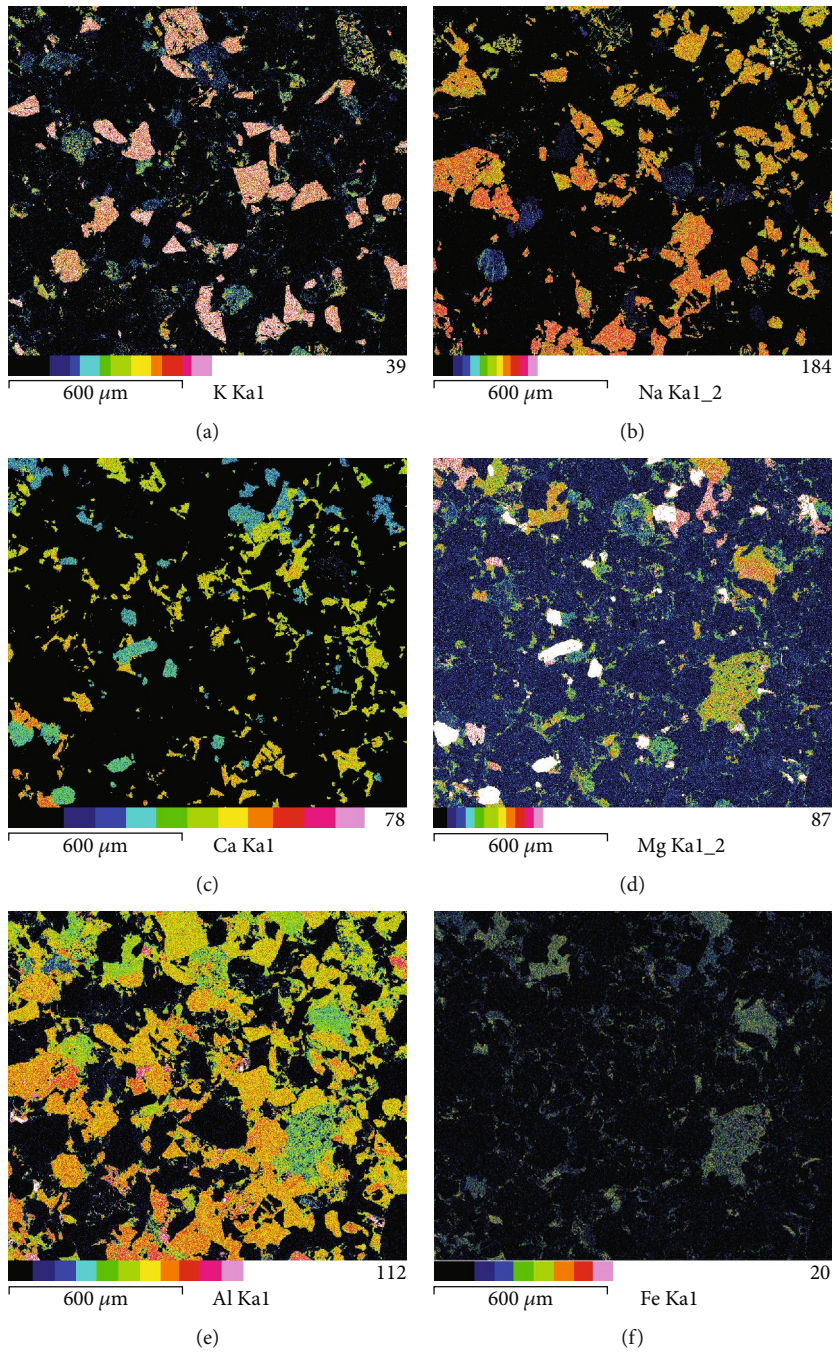

Figure 3: Continued.

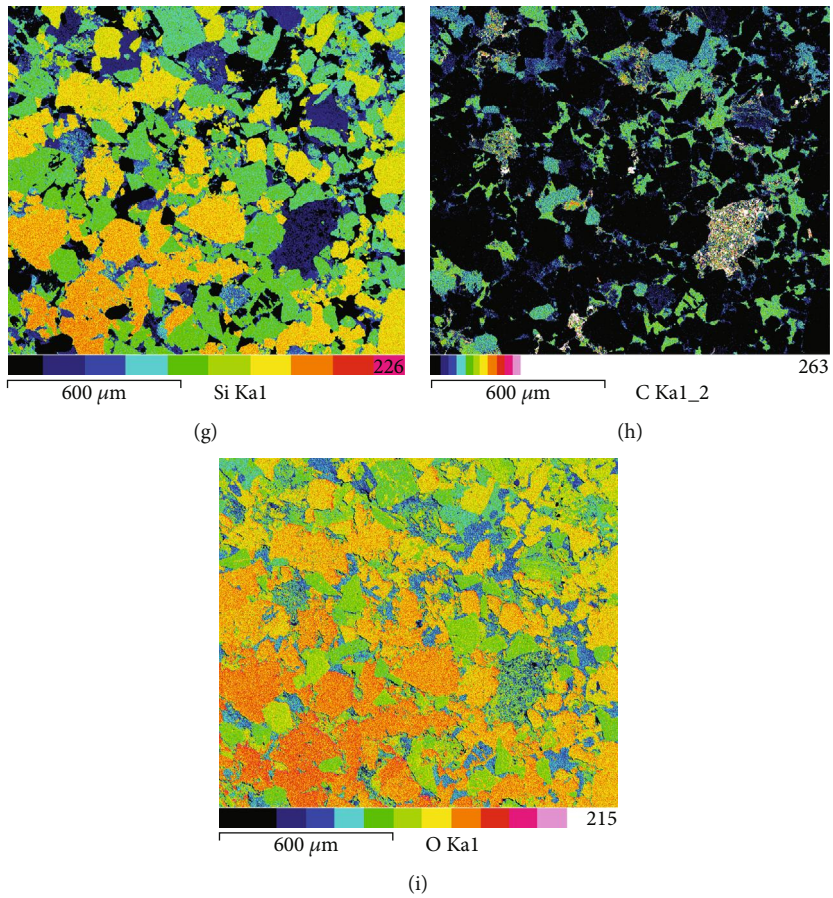

Figure 3: Sample 284-3-9-Z SEM-EDS major element distribution map: (a) K; (b) Na; (c) Ca; (d) Mg; (e) Al; (f) Fe; (g) Si; (h) C; (i) O.

and carbonate minerals. The denoise process for the skeleton mineral surface is required using marginal examination method (Figure 5). Clay minerals are relatively plastic and mainly distributed within primary pores; their morphological characteristics are closely related to the pore morphologies. Clay minerals are distributed within different types of micro-nanoscale pores, the mineral surfaces are relatively rough, and denoise is thus not required.

The SEM-EDS planar scanning element-mineral identification results are as follows (Figure 6): (1) the skeleton minerals have smooth surfaces and are widely distributed, while clay minerals are distributed within pores formed between skeleton grains; (2) the selected sample is mainly composed of skeleton minerals (quartz, albite, and potash feldspar) with proportion of 66.01%, carbonate minerals (calcite and dolomite) with 19.5%, and clay minerals (mainly chlorite and smectite and secondly kalinite and illite) with 10.59%. The proportion of pores in the selected slice is 3.78%.

Through the analysis of the minerals in the local area of the selected sample, the occurrence mode for various kinds of minerals could be clearly displayed (Figure 7). Quartz grains are developed with high content and good roundness (Figures 7(a) and 7(b)). Feldspar is mainly composed of potash feldspar and albite, and these two minerals display mutual mineral metasomatic phenomenon in many areas (Figure 7(d)), which is mainly caused by the uneven distribution of the K and Na elements in minerals. In addition, in the process of fluid filling, the albite will be dissolved into pores and filled with clay minerals and later formed carbonate minerals (Figures 7(e) and 7(f)). The clay minerals mainly attach to the surface of skeleton mineral particle and fill into large pore throats (Figures 7(c) and 7(e)).

4. Discussion

4.1. Comparison of EDS Identification and XRD Analysis. The identification results via the EDS new method are compared with the XRD mineral quantitative analyses and suggest that difference exists regarding the skeleton minerals including quartz, feldspar, carbonate, and clay minerals content, and they include the following.

(1) Quartz content: XRD analysis indicates the quartz content ranges from 25.5% to 36%, with average 30.4%, while EDS analysis indicates the quartz content ranges from 23.8% to 33.1%, with average 29.0%; the difference lies 0.3-4.8%

(2) Feldspar content: for potash feldspar, XRD analysis indicates the content ranges from 6.1% to 14.0%,

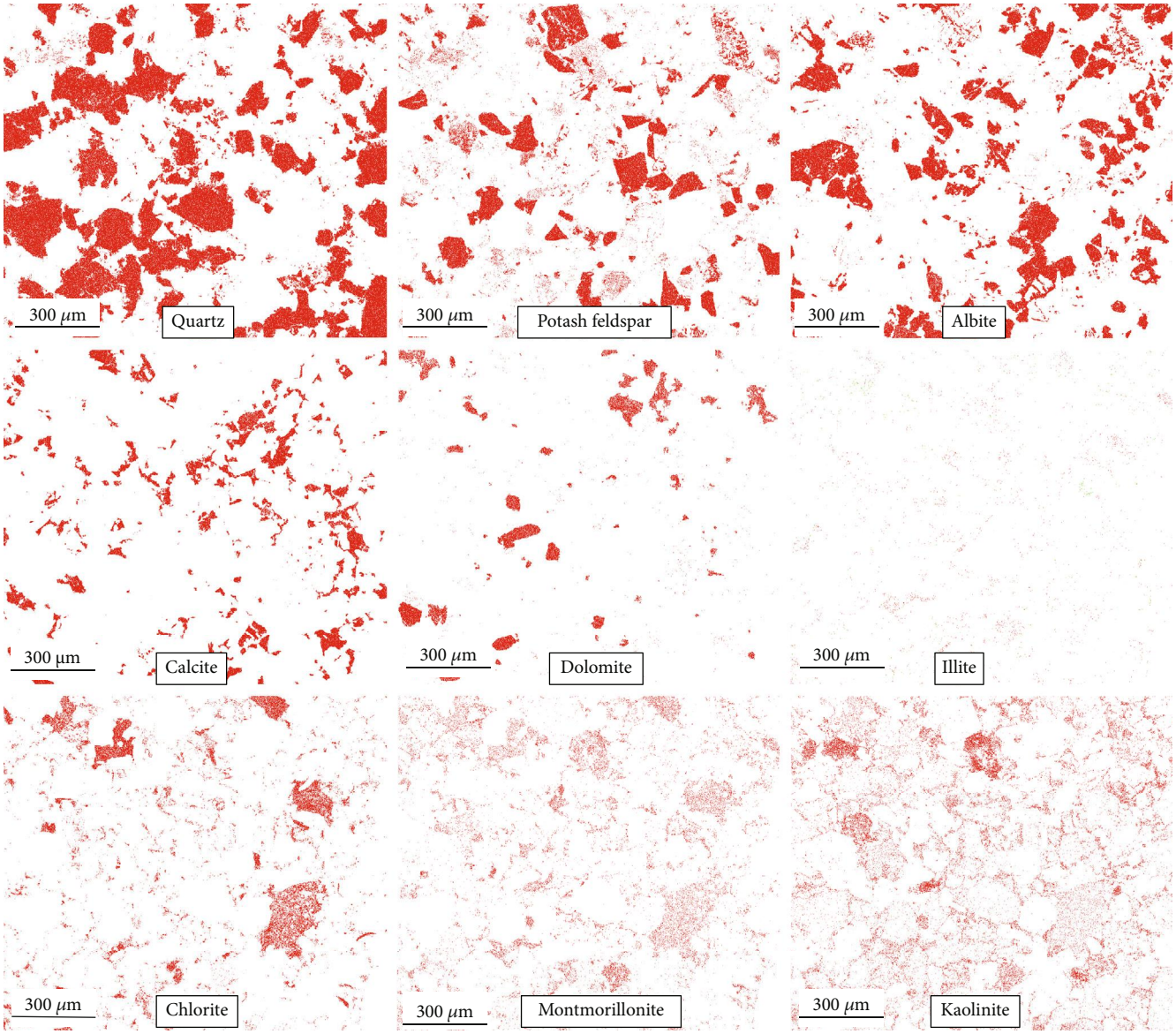

Figure 4: Sample 284-3-9-Z SEM-EDS planar scanning mineral content distribution map (before denoise).

with average 10.2%, while EDS analysis indicates the content ranges from 6.1% to 18.5%, with average 12.0%; the difference lies 0-4.5%. For albite/plagioclase: XRD analysis indicates the content ranges from 18% to 40.7%, with average 30.3%, while EDS analysis indicates the content ranges from 22% to 35%, with average 28.7%; the difference lies 1.1-5.9%

(3) Carbonate content: for calcite, XRD analysis indicates the content ranges from 0.5% to 14.2%, with average 2.4%, while EDS analysis indicates the content ranges from 0.5% to 12.1%, with average 2.9%; the difference lies 0-2.1%. For dolomite, XRD analysis indicates the content ranges from 0.8% to 13.1%, with average 7.0%, while EDS analysis indicates the content ranges from 1.8% to 11.9%, with average 7.7%; the difference lies 0-0.6-3.8%

(4) Clay minerals: XRD analysis indicates the content ranges from 11% to 36.1%, with average 19.7%, while EDS analysis indicates the content ranges from 10.7% to 33.7%, with average 19.8%; the difference lies 0-5%

In general, the content of skeleton minerals identified and calculated by the new EDS method is higher than that obtained by the XRD results (Figure 8). The reasons may include the following: (1) the new method is based on scanning electron microscopy, and skeleton minerals need to be firstly cut for sample preparation, which leads to a larger plane distribution area of skeleton minerals; (2) miscible minerals will appear identification bias, and XRD identification is based on a certain industry standard classification, which will also cause deviation; (3) the new mineral identification method can denoise the skeleton minerals and increase the surface area of the skeleton minerals.

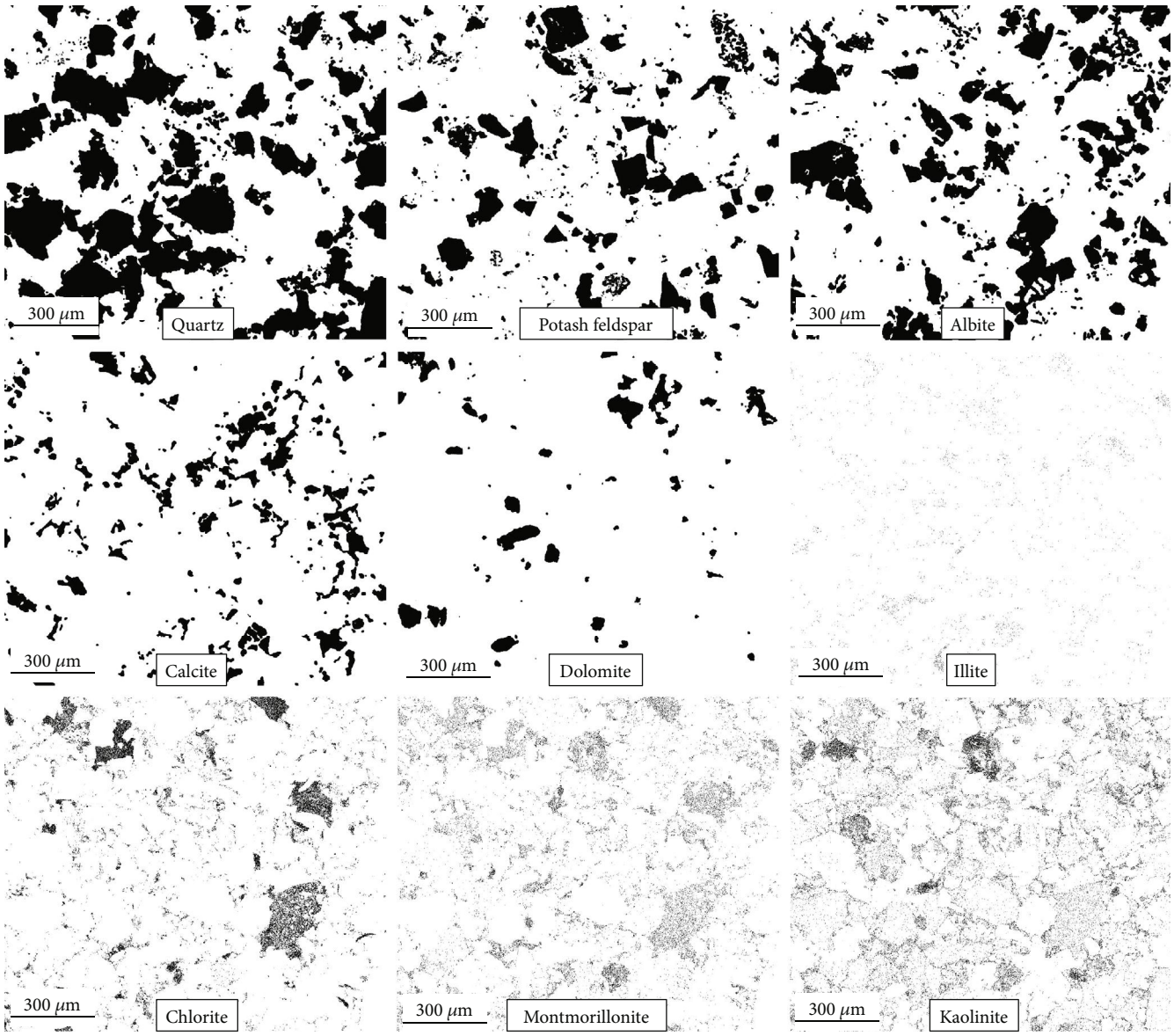

Figure 5: Sample 284-3-9-Z SEM-EDS planar scanning mineral content distribution map (after denoise).

The relative contents of clay minerals (illite, smectite, chlorite, and kaolinite) had little difference: (1) illite content: XRD content ranged from 0.9% to 10.1%, with an average of 4.5%, and EDS content ranges from 1.6% to 11%, with an average of 4.8%, with a difference of 0-2.1%; (2) smectite content: XRD content was distributed in the range of 1.9%-16.5%, with an average of 7.8%; EDS content was distributed in the range of 2%-17%, with an average of 7.4%, with a difference of 0.1-6.3%; (3) chlorite content: XRD content was 3.8%-10.2%, with an average of 7.4%, and EDS content was 3.9%-10.8%, with an average of 7.0%, with a difference of 0.1-2.4%; (4) kaolinite content: the kaolinite content in the sample area is relatively low (generally less than 1%), and XRD fails to effectively identify it. The mineral content identified by EDS is generally less than 1%, with an average content of 0.6%, and the performance of EDS identification is obviously better than that of XRD analysis.

In general, the content of clay minerals identified and calculated by the new method is higher than that analyzed by XRD (Figure 9). The reasons are perhaps as follows. (1) The new method is based on scanning electron microscopy, skeleton minerals are cut after rock slice processing, and the polishing fluid could pollute the surface characteristics of clay minerals in the reservoir, which increases the difficulty of identification. (2) After the completion of mineral identification, the new method does not denoise clay minerals, and the relative content of clay minerals may be small. (3) The minerals in the illite/smectite mixed layer cannot be effectively distinguished via the current new method.

Based on the results discussed above, the "EDS method" is able to qualitatively identify minerals, although differences exist compared to the XRD method. Advancing sampling techniques and higher resolution microscopes will reduce such differences. Meanwhile, the EDS method possess obvious

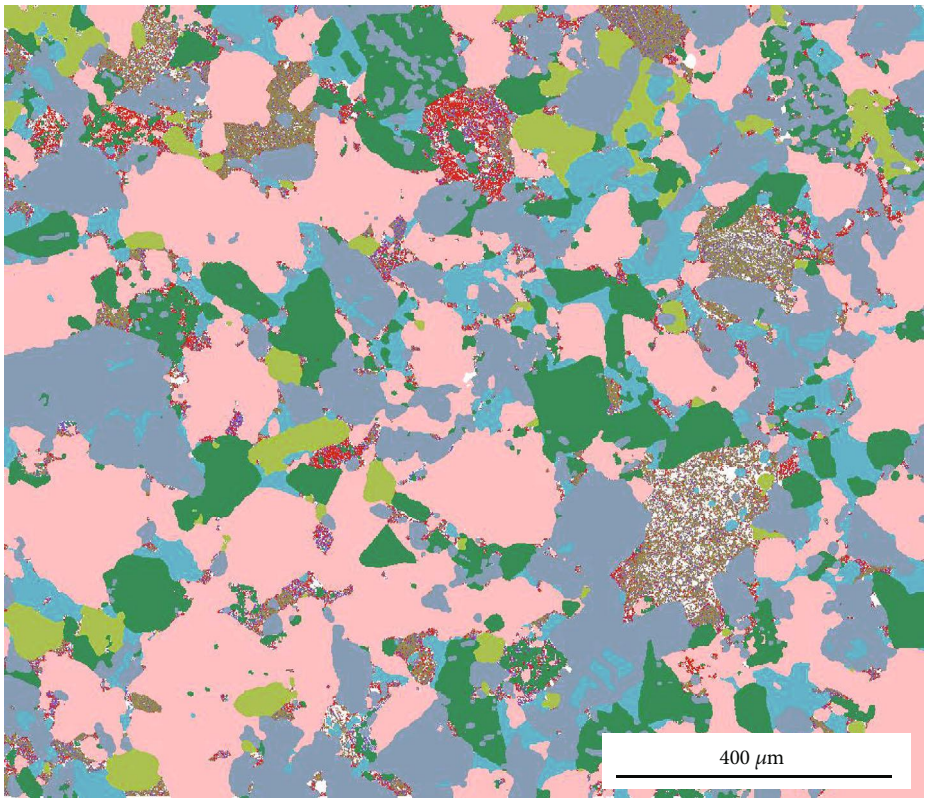

Mineral composition	Percentage content (%)
Quartz	30.86%
Potash Feldspar	10.03%
Albite	25.12%
Calcite	11.67%
Dolomite	7.60%
Siderite	0.12%
Illite	0.97%
Chlorite	4.79%
Montmorillonite	3.11%
Kaolinite	1.84%
Pore	3.89%

Figure 6: Sample 284-3-9-Z SEM-EDS planar scanning element-mineral identification result.

advantages including (1) qualitative identification and quantitative calculation are both realized through element scanning at mineral surfaces and calculating mineral content; (2) able to identify low-content minerals through element associations determination, for instance, the pyrite and siderite in this study, whereas XRD method finds it hard to identify; (3) able to identify the characteristics of miscibility minerals and calculate their content, which is of great significance to mineral characteristics and diagenesis.

4.2. EDS Identification and TIMA Analysis. The SEM-TIMA composite mineral analysis system in the School of Earth and Space Sciences, Peking University, allows analysis of microstructure and granular structure containing mineral dissociation and assemblage. This system is composed of TESCAN field emission scanning electron microscopy, TESCAN composite mineral analyzer, YAG scintillator backscattering detector BSE, and cathode fluorescence detector CL synchronous detection system [49, 50]. This system allows identification and measurement of more than 5,000 types of mineral content, through analyzing the overlap degree of mineral element spectrum, representing the cutting-edge technology [51]. The sample is also submitted to this system for analysis, and the results show that 9.68% of the area fails to recognize any minerals (Figure 10).

The sample GJ141-7-25 is analyzed via the EDS method, XRD, and TIMA method to compare the practicability. Mineral identification results obtained via the EDS method and the XRD method are similar, whereas they both display considerable differences compared to the TIMA method (Figure 11). The TIMA results rely on the standard spectrum database; to require more accurate results, it requires modification of the samples compared to the standard database. Meanwhile, although the TIMA method can identify thousands of types of minerals, it cannot identify clay minerals as accurate as the XRD and EDS methods.

4.3. "EDS Method" Advantages. The EDS method is developed on the basis of scanning electron microscopy and energy spectrum analysis in field emission environment. It is a quantitative characterization method, based on mineral element composition and pixel element combination to distinguish mineral types in microsurface areas. As a visual mineral analysis method, it has significant advantages over the XRD method. In addition to obtaining the characteristics and relative content of mineral components, this method can also display the characteristics of pore structure, which expands the characterization content of pore structure based on scanning electron microscopy and enables the micropores of oil flow with mineral properties.

The TIMA method is oriented to various rocks and multiple mineral facies of one certain mineral. In contrast, the "EDS method" is a mineral analysis method specially designed for reservoir rocks in the field of petroleum geology. By referring to XRD analysis and testing standards and other relevant industry standards in the petroleum field,

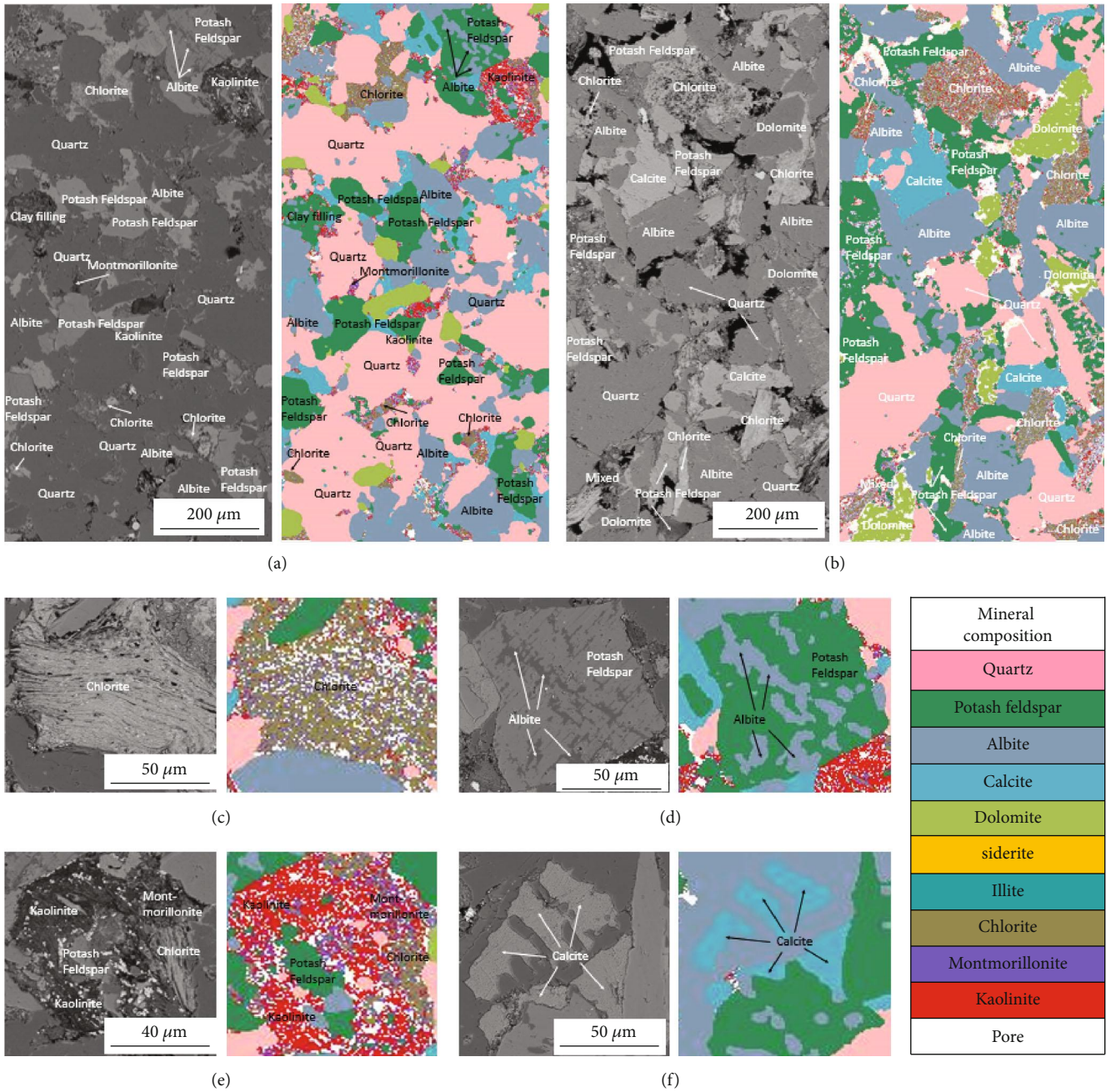

FIGURE 7: Sample 284-3-9-Z EDS element-mineral local characteristics. (a, b) Sample 284-2-45 and 284-3-9 backscatter and EDS element-mineral identification map; (c) two images of chlorite; (d) two images of potash feldspar and albite; (e) two images of major clay minerals; (f) two images of calcite.

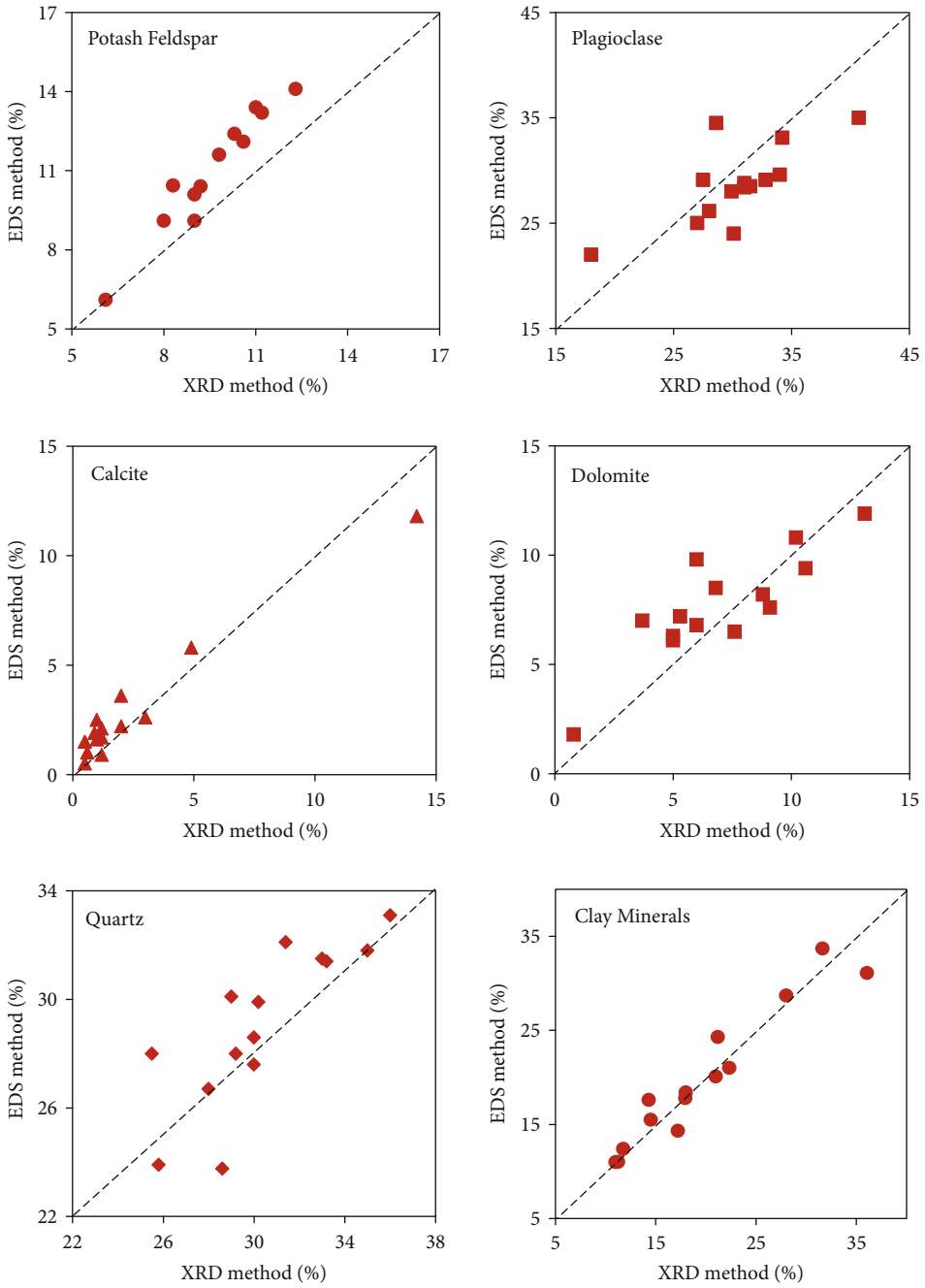

Figure 8: Skeleton mineral content results obtained via the EDS method vs. the XRD method.

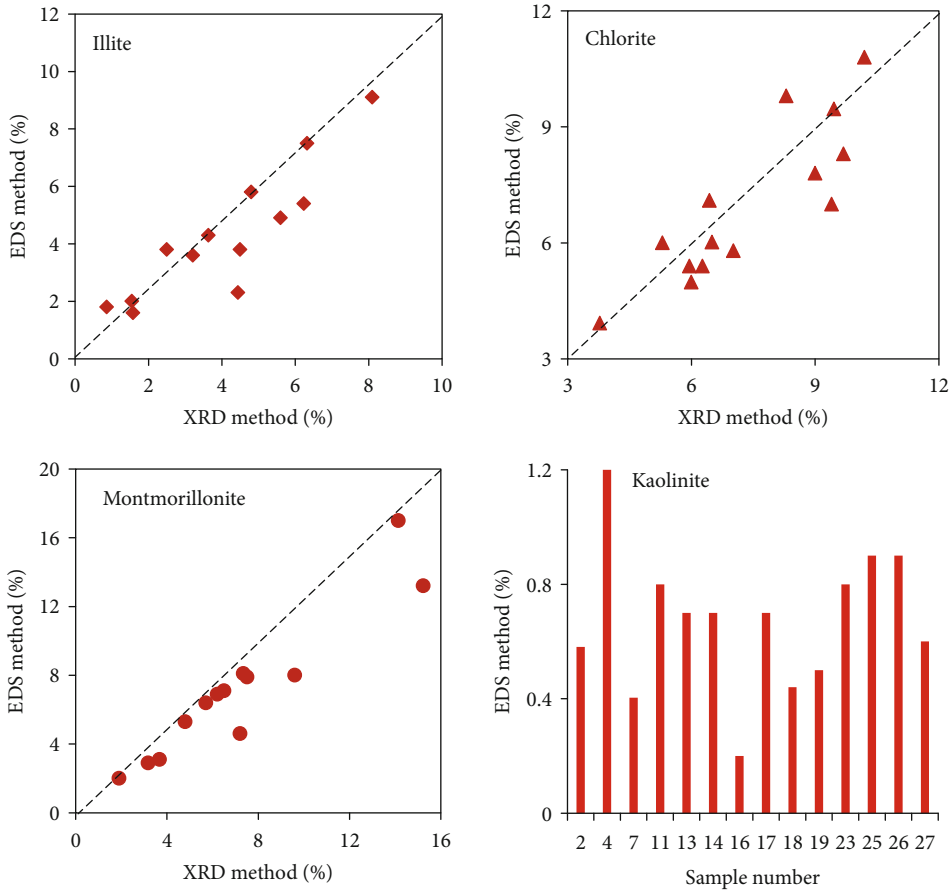

Figure 9: Clay mineral content results obtained via EDS method vs. XRD method.

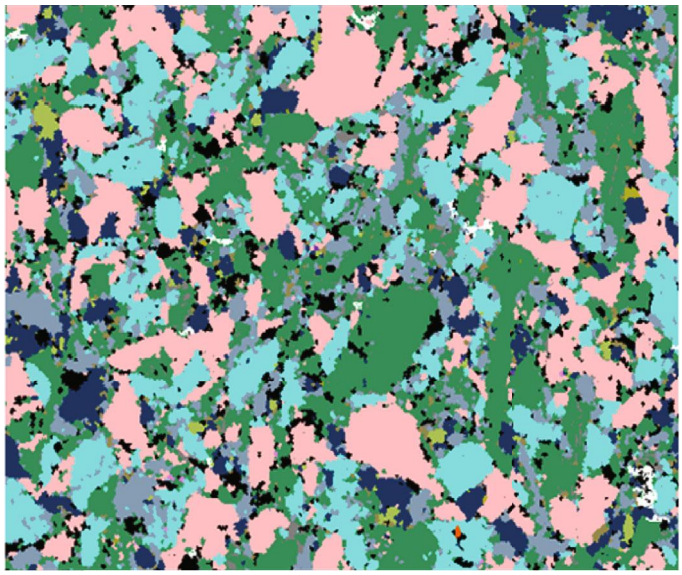

Mineral composition	Percentage content (%)
Quartz	23.86%
Orthoclase	23.29%
Plagioclase	30.01%
Calcite	8.62%
Dolomite	2.01%
Illite	1.10%
Chlorite	1.43%
Unrecognized	9.68%

Figure 10: Results obtained via SEM-TIMA method, sample Y416-3-53.

the element composition library of common minerals in various reservoirs is established to realize and strengthen the parallel comparison between various reservoir physical analysis techniques. Figure 11 shows that the EDS method analysis results are more consistent with the XRD whole-rock mineral analysis results obtained by testing under the oil

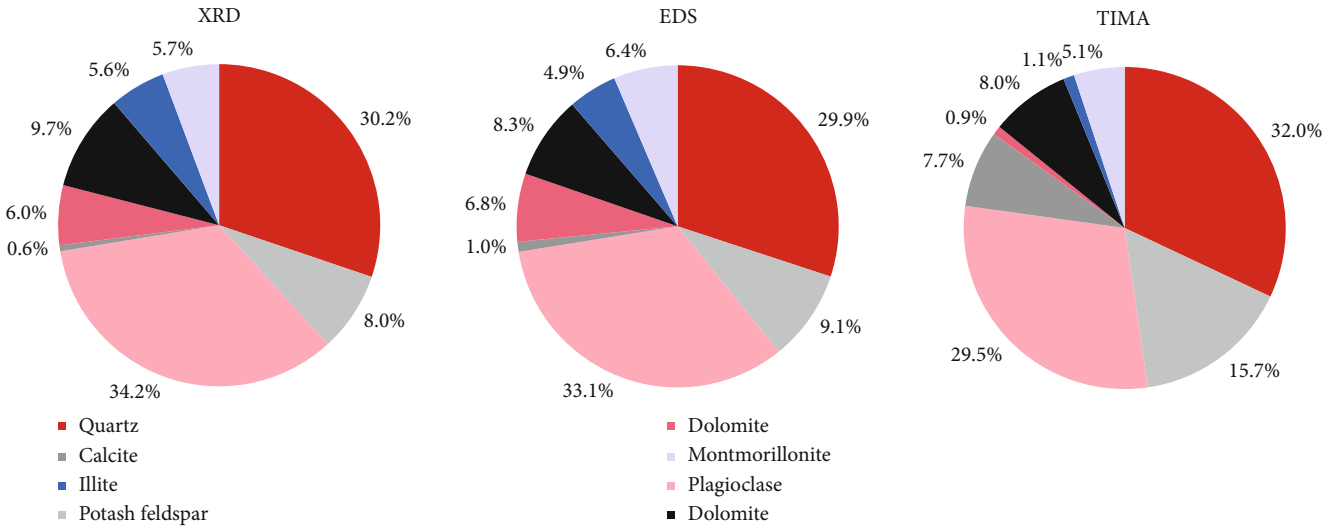

Figure 11: Results obtained via XRD, EDS method, and TIMA method, sample GJ141-7-25.

and gas industry standards. Therefore, it is also a method for coarsening mineral facies. With limited coarsening mineral facies, it focuses on the mineral component characteristics that can cause the difference of reservoir wettability and normalizes the mineral types in the reservoir, which can better serve the process of petroleum exploration and development and perhaps has stronger practical application value.

5. Conclusions

With the continuous development of hydrocarbon exploration, how to efficiently, economically, accurately, and comprehensively obtain mineral species, composition, structure, and diagenesis information has become one of the hot topics in both the academia and industry. By scanning electron microscopy (SEM) and energy dispersive spectroscopy (EDS), a new method of qualitative mineral identification and quantitative measurement is established. Typical tight sandstone reservoir rock samples in the Ordos Basin are selected; through the element surface scanning image of "mineral element composition" and "pixel element combination," mineral types are distinguished, and mineral parameters such as types, characteristics, and content are rapidly and accurately determined. Meanwhile, such results achieved via the new method are compared with those of conventional XRD and TIMA methods. The results show that the new method exhibits several advantages: cost advantages compared to XRD experiment analysis technology and TIMA system and ability to analyze low-content minerals which XRD techniques are hard to identify; it allows quantitative characterization on the phenomenon of mineral miscibility, which is of great significance to explore the mineral diagenetic evolution.

This paper proposes a new method for quantitative mineral deification, namely, the "EDS method." The main conclusions are as follows:

(1) A new method of qualitative mineral identification and quantitative measurement is established. This method employs the element surface scanning image of "mineral element composition" and "pixel element combination" to distinguish mineral types and determine mineral parameters such as types, characteristics, and content

(2) This method is applied to analyze the samples from the 6th layer of Triassic Yanchang Formation, Ordos Basin. The results show that skeleton minerals (quartz, albite, and potassium feldspar) dominate the study area, accounting for 66.01%. It also contains a lot of carbonate minerals (calcite and dolomite), accounting for 19.5%. The proportion of clay minerals is 10.59%, with chlorite and montmorillonite as the main minerals and kaolinite and illite as the second. The porosity is 3.78%, which is significantly lower than the results of physical property test, indicating that the development of clay minerals in this area played an important role in the formation of reservoir stratified pores

(3) The comparison of the "EDS method" with other methods shows that the results of the new EDS method are consistent with XRD, but there is a certain degree of deviation from the identification results of TIMA. This mainly resulted from the difference between the laboratory standard energy spectrum database established by TIMA and the actual sample. The "EDS method" is a mineral analysis method specially designed for reservoir rocks in the field of petroleum geology. Compared with XRD experimental analysis and TIMA system, the EDS method has obvious cost advantages and can better serve the process of petroleum exploration and development, suggesting potential stronger practical application value

Data Availability

The data is privileged information, not to be shared with the general public.

Conflicts of Interest

The authors declare that they have no conflicts of interest.

References

[1] C. R. Clarkson, M. Freeman, L. He et al., "Characterization of tight gas reservoir pore structure using USANS/SANS and gas adsorption analysis," *Fuel*, vol. 95, no. 1, pp. 371–385, 2012.

[2] X. Cui, A. M. M. Bustin, and R. M. Bustin, "Measurements of gas permeability and diffusivity of tight reservoir rocks: different approaches and their applications," *Geofluids*, vol. 9, no. 3, 223 pages, 2009.

[3] X. H. Yu, S. L. Li, and Z. H. Yang, "Discussion on depositon-diagenesis genetic mechanism andbot issues of tight sandstone gas reservoir," *Lithologic Reservoirs*, vol. 27, no. 1, pp. 1–13, 2015.

[4] R. K. Zhu, B. Bai, J. Cui et al., "Research advances of microstructure in unconventional tight oil and gas reserviors," *Journal of Palaeogeography*, vol. 15, no. 5, pp. 615–623, 2013.

[5] B. Li, D. Y. Liang, and L. L. Zhang, "Process mineralogy of an apatite-rich complex rare earth ore," *Journal of the chinese society of rare earths*, vol. 30, no. 6, pp. 761–765, 2012.

[6] R. D. Pascoe, M. R. Power, and B. Simpson, "QEMSCAN analysis as a tool for improved understanding of gravity separator performance," *Minerals Engineering*, vol. 20, no. 5, pp. 487–495, 2007.

[7] T. Saif, Q. Lin, A. R. Butcher, B. Bijeljic, and M. J. Blunt, "Multi-scale multi-dimensional microstructure imaging of oil shale pyrolysis using X-ray micro-tomography, automated ultra-high resolution SEM, MAPS Mineralogy and FIB-SEM," *Applied Energy*, vol. 202, pp. 628–647, 2017.

[8] B. Allard and C. Sotin, "Determination of mineral phase percentages in granular rocks by image analysis on a microcomputer," *Computers & Geosciences*, vol. 14, no. 2, pp. 261–269, 1988.

[9] G. Du, K. Y. Wang, J. Ran, F. Y. Wang, and Z. X. Pan, "Application of IR/SEM and other modern instruments for mineral identification," *Rock and mineral analysis*, vol. 33, no. 5, pp. 625–633, 2014.

[10] L. Ji, J. Qiu, Y. Q. Xia, and T. Zhang, "Micro-pore characteristics and menthane adsorption properties of common clay minerals by electron microscope scanning," *Acta Petrolei Sinica*, vol. 33, no. 2, pp. 249–256, 2012.

[11] S. J. Jiao, H. Han, Q. P. Weng, F. Yang, D. Q. Jiang, and L. S. Cui, "Scanning electron microscope analysis of porosity in shale," *Journal of Chinese Electron Microscopy Society*, vol. 31, no. 5, pp. 432–436, 2012.

[12] T. Du, Z. X. Zhou, L. M. Li, and Z. J. Zhang, "Mass effect of particle energy dispersive spectrometer quantitative analysis in scanning electron microscope," *Physical and Chemical Inspection (Physics Section)*, vol. 48, no. 6, pp. 365–369, 2012.

[13] Z. Q. Fu, J. C. Guo, C. C. He, J. Y. Zhao, and X. B. Liu, "Studies on standardization of nanometer scale measurement by SEM," *Standard Science*, vol. 3, pp. 34–37, 2012.

[14] J. Workman and J. L. Weyer, "Practical guide to interpretive near infrared spectroscopy," Chemical Industry Press, Beijing, 2009.

[15] Y. Li, Y. P. Wang, C. Y. Zhao, and L. U. JL, "The FTIR study on structure changes of coal kerogen in the maturation process," *Bulletin of Mineralogy, Petrology and Geochemistry*, vol. 32, no. 1, pp. 97–101, 2013.

[16] S. Cheng, J. Cao, Y. Li, G. Hu, and Z. Yi, "TEM observations of particles in groundwater and their prospecting significance in the Bofang copper deposit, Hunan, China," *Ore Geology Reviews*, vol. 95, pp. 382–400, 2018.

[17] G. Hu, J. Cao, and T. Jiang, "Discovery and prospecting significance of metal-bearing nanoparticles within natural invertebrate tissues," *Ore Geology Reviews*, vol. 99, pp. 151–165, 2018.

[18] Y. L. Zou, Q. L. Huo, and X. Yu, "The analytical technique of the micro infrared spectra of the hydrocarbon inclusions and its application," *Bulletin of Mineralogy, Petrology and Geochemistry*, vol. 25, no. 1, pp. 105–108, 2006.

[19] M. C. He and Z. J. Zhang, "The application of laser Raman microspectroscopy to study of mineral deposits," *Rock and mineral analysis*, vol. 20, no. 1, pp. 43–46, 2001.

[20] Y. H. Huang, *Quantitative Reserch of Fluid Inclusions by Laser Raman and Infrared Spectroscopy*, China University of Geosciences, 2018.

[21] T. P. Mernagh and A. R. Wilde, "The use of the laser Raman microprobe for the determination of salinity in fluid inclusions," *Geochimica et Cosmochimica Acta*, vol. 53, no. 4, pp. 765–771, 1989.

[22] J. D. Pasteris, C. A. Kuehn, and R. J. Bodnar, "Applications of the laser Raman microprobe RAMANOR UH000 to hydrothermal ore. deposits; Carlin as an example," *Economic Geology*, vol. 81, no. 4, pp. 915–930, 1986.

[23] G. J. Rosasco, E. Roedder, and J. H. Simmons, "Laser- excited Raman spectroscopy for nondestructive partial analysis of individual phases in fluid inclusions in minerals," *Science*, vol. 190, no. 4214, pp. 557–560, 1975.

[24] M. Futamata, P. Borthen, J. Thomassen, D. Schumacher, and A. Otto, "Application of an ATR method in Raman spectroscopy," *Applied Spectroscopy.*, vol. 48, no. 2, pp. 252–260, 1994.

[25] F. Ni, L. Thomas, and T. M. Cotton, "Surface-enhanced resonance Raman spectroscopy as an ancillary high-performance liquid chromatography detector for nitrophenol compounds," *Analytical Chemistry*, vol. 61, no. 8, pp. 888–894, 1989.

[26] E. Roth and W. Kiefer, "Surface-enhanced Raman spectroscopy as a detection method in gas chromatography," *Applied Spectroscopy*, vol. 48, no. 10, pp. 1193–1195, 1994.

[27] D. A. Stuart, C. R. Yonzon, X. Zhang et al., "Glucose sensing using near-infrared surface-enhanced Raman spectroscopy: gold surfaces, 10-day stability, and improved accuracy," *Analytical Chemistry*, vol. 77, no. 13, pp. 4013–4019, 2005.

[28] H. P. Klug and L. E. Alexander, "X-ray diffraction procedures: for polycrystalline and amorphous materials," John Wiley & Sons, New York, 2nd edition, 1974.

[29] Y. F. Hao and A. L. Zhao, "A simple method of quantitative analysis for calcite and dolomite in rock by X-ray diffraction," *Non-ferrous mining and metallurgy*, vol. 21, no. 5, pp. 61–63, 2005.

[30] Q. Q. Zhong, S. J. Huang, M. L. Zou, H. P. Tong, K. K. Huang, and X. H. Zhang, "Controlling factors of order degree of dolomite in carbonate rocks: a case study from Lower Paleozoic in Tahe Oilfield and Triassic in northeastern Sichuan Basin," *Lithologic reservoirs*, vol. 21, no. 3, pp. 50–55, 2009.

[31] G. C. Chi, L. H. Song, N. Wang, D. S. Cui, and G. X. Zhou, "Identification of alteration mineral composition of kimberlite from Shandong Mengy by X-ray powder diffractometer," *Rock and mineral analysis*, vol. 29, no. 4, pp. 475–477, 2010.

[32] G. C. Chi, G. Xiao, Y. L. Chen et al., "Application of X-ray powder diffractometer in the identification and classification of phyllite," *Geology and resources*, vol. 22, no. 5, pp. 409–414, 2013.

[33] X. L. Pang, X. C. Liu, and Y. Xue, "Application of powder X-ray diffraction in petrology and mineralogy," *Rock and mineral analysis*, vol. 28, no. 5, pp. 452–456, 2009.

[34] M. Redwan, D. Rammlmair, and J. A. Meima, "Application of mineral liberation analysis in studying micro-sedimentological structures within sulfide mine tailings and their effect on hardpan formation," *Science of the Total Environment*, vol. 414, pp. 480–493, 2012.

[35] Y. Liu, R. Gupta, A. Sharma et al., "Mineral matter-organic matter association characterisation by QEMSCAN and applications in coal utilisation," *Fuel*, vol. 84, no. 10, pp. 1259–1267, 2005.

[36] T. S. Song, X. Li, Y. Zhang et al., "QEMSCAN mineral quantitative analysis of tight sandstone diagenesis in Fuyu oil layer, Daqing Placanticline," *Geological Science and Technology Information*, vol. 35, no. 3, pp. 193–198, 2016.

[37] L. G. Wen, P. S. Zeng, and X. C. Zhan, "Application of the automated mineral identification and characterization system (AMICS) in the identification of rare earth and rare minerals," *Rock and Mineral Analysis*, vol. 37, no. 2, pp. 121–129, 2018.

[38] R. A. Creelman and C. R. Ward, "A scanning electron microscope method for automated, quantitative analysis of mineral matter in coal," *International Journal of Coal Geology*, vol. 30, no. 3, pp. 249–269, 1996.

[39] P. Ying and H. D. Yu, "Application of synthetic energy dispersive spectra(Eds) to identification and search of uncommon mineral," *Mining and Metallurgy*, vol. 14, no. 3, pp. 83–86, 2005.

[40] K. Guanira, T. M. Valente, C. A. Ríos et al., "Methodological approach for mineralogical characterization of tailings from a Cu(Au,Ag) skarn type deposit using QEMSCAN (quantitative evaluation of minerals by scanning electron microscopy)," *Journal of Geochemical Exploration*, vol. 209, p. 106439, 2020.

[41] X. Li, Y. Li, J. Li et al., "Characteristics of pore structures from the Lower Paleozoic shale gas reservoirs in northern Guizhou, South China," *Journal of Natural Gas Geoscience*, vol. 5, no. 5, pp. 241–253, 2020.

[42] Z. Liu, D. Liu, Y. Cai, and Y. Qiu, "Permeability, mineral and pore characteristics of coals response to acid treatment by NMR and QEMSCAN: insights into acid sensitivity mechanism," *Journal of Petroleum Science and Engineering*, vol. 198, p. 108205, 2021.

[43] A. M. Nazari, A. Ghahreman, and S. Bell, "A comparative study of gold refractoriness by the application of QEMSCAN and diagnostic leach process," *International Journal of Mineral Processing*, vol. 169, pp. 35–46, 2017.

[44] L. Santoro, M. Boni, G. K. Rollinson, N. Mondillo, G. Balassone, and A. M. Clegg, "Mineralogical characterization of the Hakkari nonsulfide Zn(Pb) deposit (Turkey): the benefits of QEMSCAN®," *Minerals Engineering*, vol. 69, pp. 29–39, 2014.

[45] M. U. Shafiq, H. K. Ben Mahmud, and M. Arif, "Mineralogy and pore topology analysis during matrix acidizing of tight sandstone and dolomite formations using chelating agents," *Journal of Petroleum Science and Engineering*, vol. 167, pp. 869–876, 2018.

[46] F. L. da Silva, G. F. Moreira, K. S. Pires, F. L. von Kruger, and F. G. da Silva Araujo, "Quantitative phases characterization of clayey ceramics containing manganese ore tailings," *Journal of Materials Research and Technology*, vol. 9, no. 5, pp. 11884–11894, 2020.

[47] X. Tang, Z. Jiang, S. Jiang, and Z. Li, "Heterogeneous nanoporosity of the Silurian Longmaxi Formation shale gas reservoir in the Sichuan Basin using the QEMSCAN, FIB-SEM, and nano-CT methods," *Marine and Petroleum Geology*, vol. 78, pp. 99–109, 2016.

[48] A. D. Van Rythoven, K. Pfaff, and J. G. Clark, "Use of QEMSCAN® to characterize oxidized REE ore from the Bear Lodge carbonatite, Wyoming, USA," *Ore and Energy Resource Geology*, 2020, article 100005.

[49] A. Beinlich, T. John, J. C. Vrijmoed, M. Tominaga, T. Magna, and Y. Y. Podladchikov, "Instantaneous rock transformations in the deep crust driven by reactive fluid flow," *Nature Geoscience*, vol. 13, no. 4, pp. 307–311, 2020.

[50] Q. Chen, W. L. Song, J. K. Yang et al., "Principle of automated mineral quantitative analysis system and its application in petrology and mineralogy: an example from TESCAN TIMA," *Mineral Deposits*, vol. 40, no. 2, pp. 345–368, 2021.

[51] T. Hrstka, P. Gottlieb, R. Skála, K. Breiter, and D. Motl, "Automated mineralogy and petrology - applications of TESCAN Integrated Mineral Analyzer (TIMA)," *Journal of Geosciences*, vol. 63, pp. 47–63, 2018.